CALPHAD optimization of SiO_2-B_2O_3-Al_2O_3-ZnO-CaO-Na_2O-Li_2O-MoO_3 system and their applications to high-level radioactive waste vitrification

Toru Sgawara[1)], Toshiaki Ohira[1)], Kohei Owaku[2)], Norio Kanehira[2)], Takeshi Tsukada[2)]

1) Akita University, 2) Japan Nuclear Fuel Limited

1. Introduction

In vitrification of high-level radioactive waste, molybdenum (Mo) contained as a fission product tends to separate into a low-viscosity fluid called the yellow phase in cold cap when the waste loading is high (**Fig. 1**). The occurrence of yellow phase is attributed to phase separation of the Mo phase in the borosilicate melt. The yellow phase can incorporate various radioactive elements and is highly water-soluble. It is necessary to understand the behavior of molybdenum in borosilicate melts in order to develop glass matrix with sufficient chemical durability and high waste loading.

We carried out the phase equilibrium experiments in the system SiO_2-Na_2O—MoO_3 and SiO_2-B_2O_3-Al_2O_3-ZnO-CaO-Na_2O-Li_2O-MoO_3 at 1200°C and 1000°C (**Figs. 4, 5 and 6**). Element partitioning between phase-separated silicate liquid and molybdate liquid (simulated yellow phase) were determined. By combining new phase equilibrium data, phase relation of SiO_2-free MoO_3-bearing system and thermodynamic data of MoO_3-bearing solid phase, the internally-consistent thermodynamic database (**Tables 2, 3 and 4**) were developed to calculate phase separation of Mo-rich alumino-borosilicate liquid by means of the CALculation of PHAse Diagram (CALPHAD) technique. The database allows us to calculate phase relation of MoO_3-bearing borosilicate systems and to predict ability of saturation and crystallization of molybdenum phase under equilibrium condition.

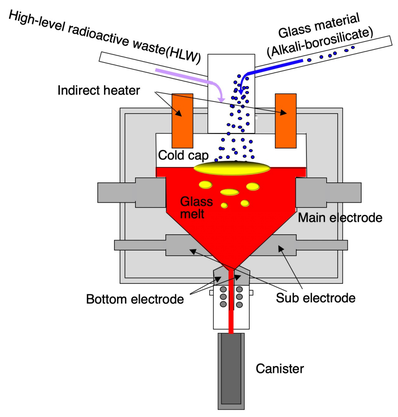

Figure 1. Schematic figure showing liquid-fed joule-heated ceramic melter (LFCM) in Rokkasho Reprocessing Plant, Japan.

4. Application and Summary

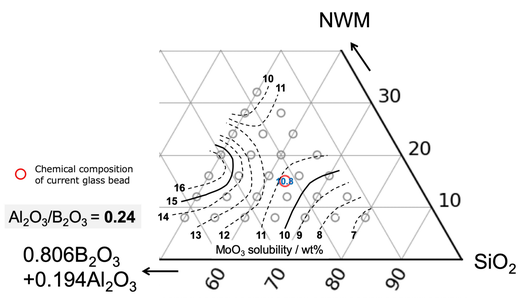

Figure 11. Compositional dependence of MoO_3 solubility (wt%) at 1200°C calculated using thermodynamic database in the pseudo ternary system SiO_2-(B_2O_3+Al_2O_3)-Network modifier component.

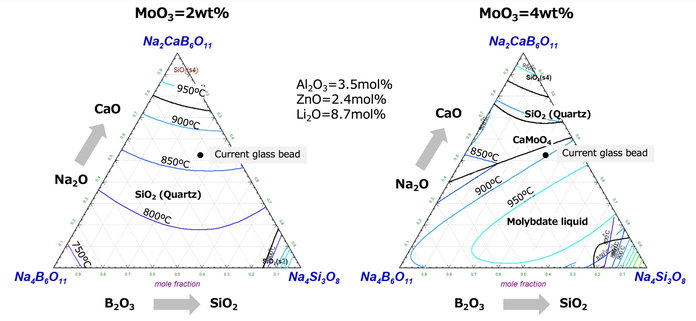

Figure 12. Liquidus phase diagram around current glass bead composition at MoO_3=2wt% and 4wt% calculated using thermodynamic database.

- We found that liquid-liquid immiscibility of SiO_2-Na_2O-MoO_3 system is less expanded than that reported previously (**Fig. 4**).
- The MoO_3 solubility depends on the degree of polymerization and the Na_2O activity of silicate liquid (**Fig. 6**).
- Thermodynamic database of MoO_3-bearing alumino-borosilicate systems was developed (**Tables 2, 3 and 4**).
- The MoO_3 solubility of current glass bead and their compositional dependence can be calculated using thermodynamic database (**FIg. 11**).

2. Experimental

2-1. Method

The mixtures of raw materials (SiO_2, B_2O_3, Al_2O_3, ZnO, Na_2CO_3, $CaCO_3$, Li_2CO_3, MoO_3) was put in a platinum crucible

↓

Heating in furnace at 1200 or 1000 °C for 24 h in air

↓

Quenched by water

↓

Analysis of chemical composition of **glass** and **precipitate** by EPMA, XRF and ICP-AES

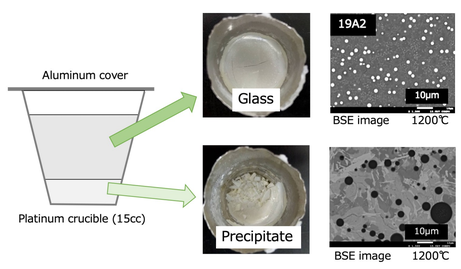

Figure 2. Appearance and back-scattered image of quenched samples. White droplet in glass is powellite ($CaMoO_4$) or Na_2MoO_4 crystallized under cooling stage.

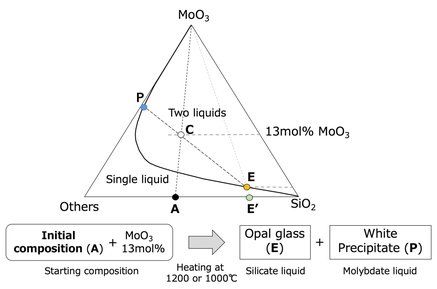

Figure 3. Schematic phase diagram showing relationship between initial composition (**C**) and two liquids (**E** and **P**) by phase separation in quenched sample. MoO_3 content in the E equals saturaton solubility for composition **E'**.

Starting composition (**A**) : **s**[(1-**x**-**y**-**p**)SiO_2-**x**B_2O_3-**y**Al_2O_3-**p**ZnO]-(1-**s**)[(1-**z**-**q**)Na_2O-**z**CaO-**q**Li_2O]

Composition range in 8 oxide component system:
s=0.63-0.80, x=0.19-0.40, y=0.01-0.10, p=0.03-0.07, z=0.10-0.35, q=0.10-0.60.
13mol% or 15mol% MoO_3 was added for all composition.

Number of experiments : SiO_2-Na_2O-MoO_3=21, 8 oxide system=94.

2-2. Results

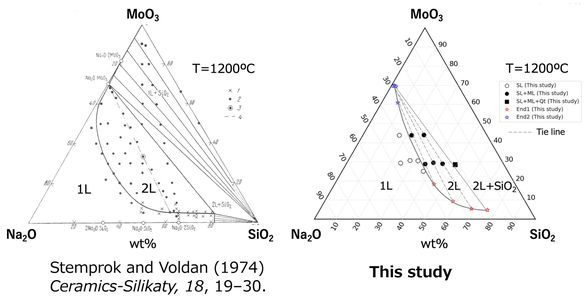

Figure 4. Comparison of phase relationships in the system SiO_2-Na_2O-MoO_3 by this study and previous report.

Our experimental results revealed that the liquid-liquid immiscibility in the SNM system is clearly smaller than that reported by Stemprok and Voldan (1974) (**Fig. 4**). The MoO_3 solubility in 8 component system increased with decreasing melt viscosity and Na_2O activity at constant temperature (**Fig. 6**).

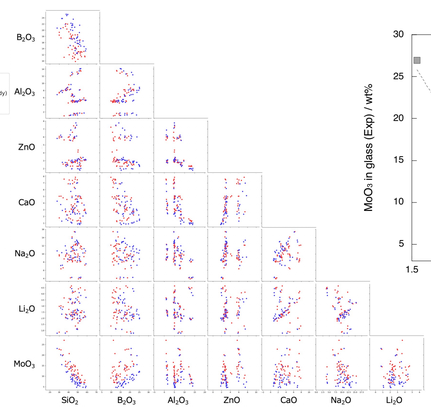

Figure 5. Chemical compostition (wt%) of MoO_3 saturated silicate liquid. Red : 1200°C, Blue : 1000°C

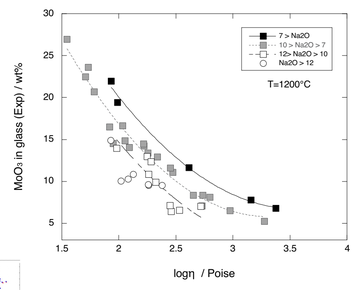

Figure 6. Relationship between MoO_3 solubility in 8 component system and log viscosity of liquid at 1200°C.

3. CALPHAD optimization

3-1. Thermodynamics

Gibbs energy of liquid is calculated from sum of liquid components (i) and Gibbs energy of mixing

$$G^{Liquid} = \sum_i x_i G_i^{\circ} + G_{Mix} \quad (1)$$

Then the mole fraction, x_i was determined by assuming associate species model. The Na_2MoO_4, $CaMoO_4$, Zn_2MoO_4 and Li_2MoO_4 were assumed for associate species in MoO_3-bearing multicomponent liquids.

The liquid-liquid immiscibility is caused by positive enthapy of mixing (H_{Mix}) of liquid phase (**Fig. 7**). The H_{Mix} was approximated by Redlich–Kister polynomial,

$$G_{Mix} = H_{Mix} - TS_{Mix}$$

$$= \sum_i \sum_j x_i x_j \sum_a L_{ij}^a (x_i - x_j)^a + RT \sum_i x_i ln x_i \quad (2)$$

We used **AKITBASE** to calculate the G^{Liquid} of SiO_2-B_2O_3-Al_2O_3-ZnO-CaO-Na_2O-Li_2O system.

The interaction parameters, L_{ij} for the SiO_2-free MoO_3-bearing system (**Table 2**) and SiO_2-Na_2O-MoO_3 system (**Table 3**) were determined by combining phase relationship and thermodynamic data of solid phase. Then, L_{ij} for interaction between alumino-borosilicate components and Mo-associate species (n=52, **Table 4**) were determined based on the 2510 constraints to minimize square sum of residuals between the calculated and the experimental values in phase separated components. All calculation were performed using FACTSage by CRCT and GTT-Technologies.

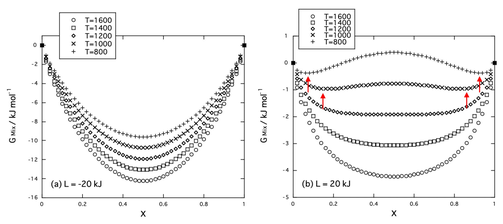

Negative enthalpy of mixing
→ Single minimum value of G_{mix}

Positive enthalpy of mixing
→ Two local minimuns of G_{mix} at low temperature
→ **Liquid-liqud immiscibility**

Figure 7. Gibbs energy of mixing and phase separation in the case of positive and negative interaction parameters.

Table 1. Thermodynamic database and optimized parameters of molybdenum-bearing silicate liquid.

		Component *j*				
		Species of glass components	Associate species of molybdenum component			
		SiO_2-B_2O_3-Al_2O_3-ZnO-CaO-Na_2O-Li_2O	Na_2MoO_4	$CaMoO_4$	Zn_2MoO_4	Li_2MoO_4
		Optimized based on the phase equilibrium data				
Component *i*	SiO_2	**AKITBASE** developed by GTT Technologies	**SiO_2-Na_2O-MoO_3** system (**Table 3**)	**SiO_2-B_2O_3-Al_2O_3-ZnO-Na_2O-CaO-Li_2O-MoO_3** system (Aumino-borosilicate system, **Table 4**)		
	B_2O_3					
	Al_2O_3					
	ZnO					
	Li_2O		**Na_2O-CaO-Li_2O-ZnO-MoO_3** system (SiO_2-free system, **Table 2**)			
	CaO					
	Na_2O					

3-2. Na_2O-CaO-Li_2O-ZnO-MoO_3 system

Table 2. Interaction parameters for SiO_2-free MoO_3-bearing liquid.

Interaction parameter L_{ij}				
i	*j*	a=0	a=1	a=2
Mo_2O_6	Na_2MoO_4	-161000+80T	-10000	0
Mo_2O_6	$CaMoO_4$	-59000	-10000	30000
Na_2MoO_4	$CaMoO_4$	-10500	-5500	-8000
B_2O_3	Mo_2O_6	-14000	-12000	-6000
Mo_2O_6	ZnO	-27000	-8000	0
ZnO	$ZnMoO_4$	-46000	0	0
Li_2O	Li_2MoO_4	10000	0	0
Mo_2O_6	Li_2MoO_4	-75000	0	0
Li_2MoO_4	ZnMoO4	-31000	8000	15000
$BLiO_2$	Li_2MoO_4	15000	0	6000
$Li_2B_4O_7$	Mo_2O_6	-50000	0	0
$Li_2B_4O_7$	Li_2MoO_4	12000	-28000	0
Na_2MoO_4	Li_2MoO_4	-11000	-3000	0
$CaMoO_4$	Li_2MoO_4	-10000	0	0
Na_2MoO_4-$CaMoO_4$	Li_2MoO_4	-80000	0	0
$CaMoO_4$-Li_2MoO_4	Na_2MoO_4	-80000	0	0
Li_2MoO_4-Na_2MoO_4	$CaMoO_4$	-80000	0	0

Figure 8. Comparison between experimental and calculated phase relationship of SiO_2-free MoO_3-bearing systems.

3-3. SiO_2-Na_2O-MoO_3 system

Table 3. Interaction parameters for SiO_2-Na_2O-MoO_3 liquid.

Interaction parameter L_{ij}				
i	*j*	a=0	a=1	a=2
Si_2O_4	Mo_2O_6	70000	0	0
Si_2O_4	Na_2MoO_4	55000	0	0
$Na_2Si_2O_5$	Na_2MoO_4	44000	-5000	0
$Na_2Si_4O_6$	Na_2MoO_4	12000	0	10000
$Na_2Si_8O_8$	Na_2MoO_4	7000	-12000	0

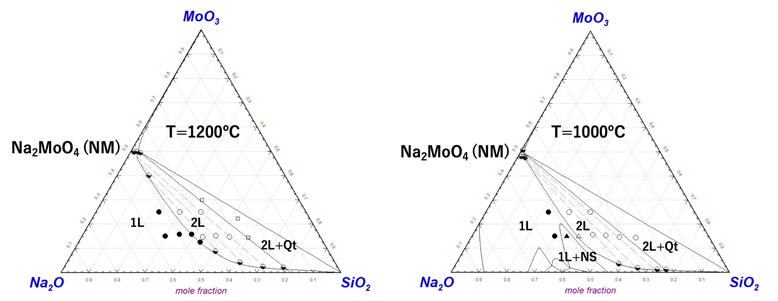

Figure 9. Experimental and calculated phase relationship in the system SiO_2-Na_2O-MoO_3 at 1200°C and 1000°C.

3-4. SiO_2-B_2O_3-Al_2O_3-ZnO-CaO-Na_2O-Li_2O-MoO_3 system

Table 4. Interaction parameters for alumino-borosilicate liquid.

		Interaction parameter L_{ij}				
		Component *j*				
Component *i*	*a*	Mo_2O_6	Na_2MoO_4	$CaMoO_4$	Li_2MoO_4	Zn_2MoO_4
Si_2O_4	0	70000	**Table 3**	-7000	77000	-90000
$Si_2Na_2O_5$	0	70000	**Table 3**	37000	48000	10000
$Si_2Na_4O_6$	0	70000			150000	150000
$CaSiO_3$	0	70000	120000	35000	150000	147000
B_2O_3	0	**Table 2**	-11000	-10000	7000	-207000
$BNaO_2$	0	-20000	98000	-12000	54000	12000
$B_4Na_2O_7$	0	-20000	28000		19000	-86000
$BNaO_2$	1		121000			
$B_4Na_2O_7$	1		11000			
$BNaO_2$	2		150000			
$B_4Na_2O_7$	2		150000			
B_2CaO_4	0	-20000				
B_4CaO_7	0	-20000	120000	64000	150000	147000
$B_2Ca_2O_5$	0	-20000				
$Si_2Al_2Na_2O_8$	0	70000	24000	33000	10000	-38000
$Si_6Al_2Na_2O_{16}$	0	70000				
$Ca_3Na_2Si_6O_{16}$	0	0	150000	150000		
ZnB_2O_4	0	-20000	27000	-8000	2000	-128000
$Li_2Si_2O_5$	0	70000	-22000	-30000	98000	-141000
Li_2SiO_3	0	70000	6000			
$BLiO_2$	0	-20000	30000	-16000	**Table 2**	-107000
$B_4Li_2O_7$	0	**Table 2**	60000			
$LiAlSiO_4$	0	70000	-26000	138000		
$LiAlSi_2O_6$	0	70000				

Table 5. Comparison of element partitioning between experimental and calculated immiscible liquids at 1200ºC for the data not used to calibrate interaction parameters.

	Initial composition / mass %	*Silicate liquid*		*Molybdate liquid*	
		Exp.	**Calc.**	Exp.	**Calc.**
SiO_2	39.82	39.07	38.87	0.75	0.94
B_2O_3	9.48	9.22	8.90	0.23	0.56
Al_2O_3	4.10	4.21	4.04	0.01	0.18
ZnO	2.45	2.46	2.30	0.14	0.30
CaO	4.37	3.59	2.80	0.86	1.65
Na_2O	13.98	9.49	10.24	4.22	3.47
Li_2O	3.19	2.35	1.95	0.73	1.13
MoO_3	22.62	7.48	5.88	15.19	16.79
Total	100.00	77.87	74.98	22.13	25.02

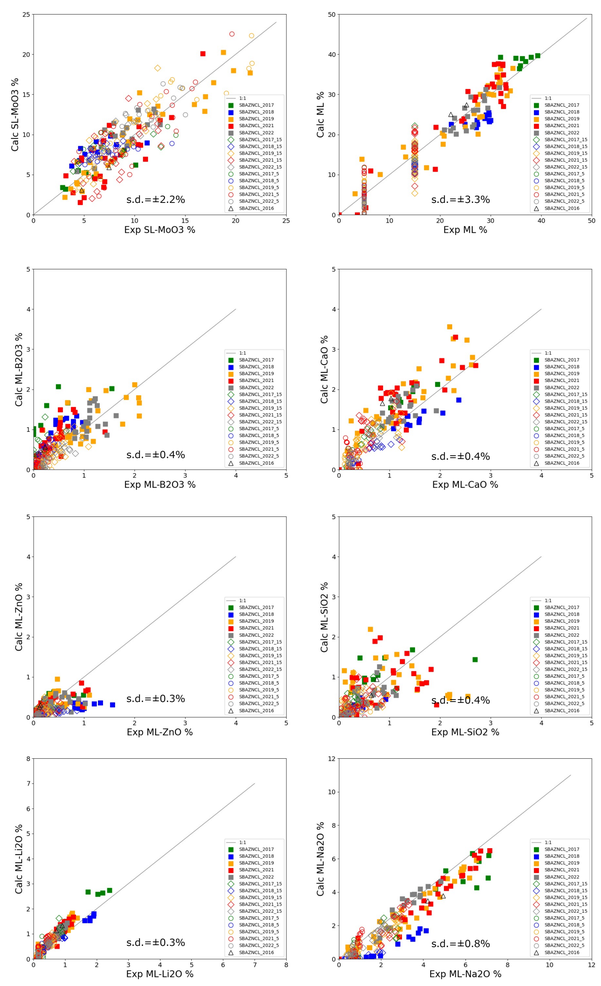

Figure 10. Comparison between calculated and experimental MoO_3 solubility in silicate liquid and components in molybdate liquid (ML).

ACKNOWLEDGEMENT

This work was carried out as a part of the basic research programs of vitrification technology for waste volume reduction (JPJ010599) supported by the Ministry of Economy, Trade and Industry, Japan.